Elastic biodegradable starch/ethylene-co-vinyl alcohol fibre-mesh scaffolds for tissue engineering applications

Journal:	*Journal of Applied Polymer Science*
Manuscript ID:	APP-2013-10-3525.R1
Wiley - Manuscript type:	Research Article
Keywords:	biodegradable, biomaterials, porous materials, mechanical properties, elastomers

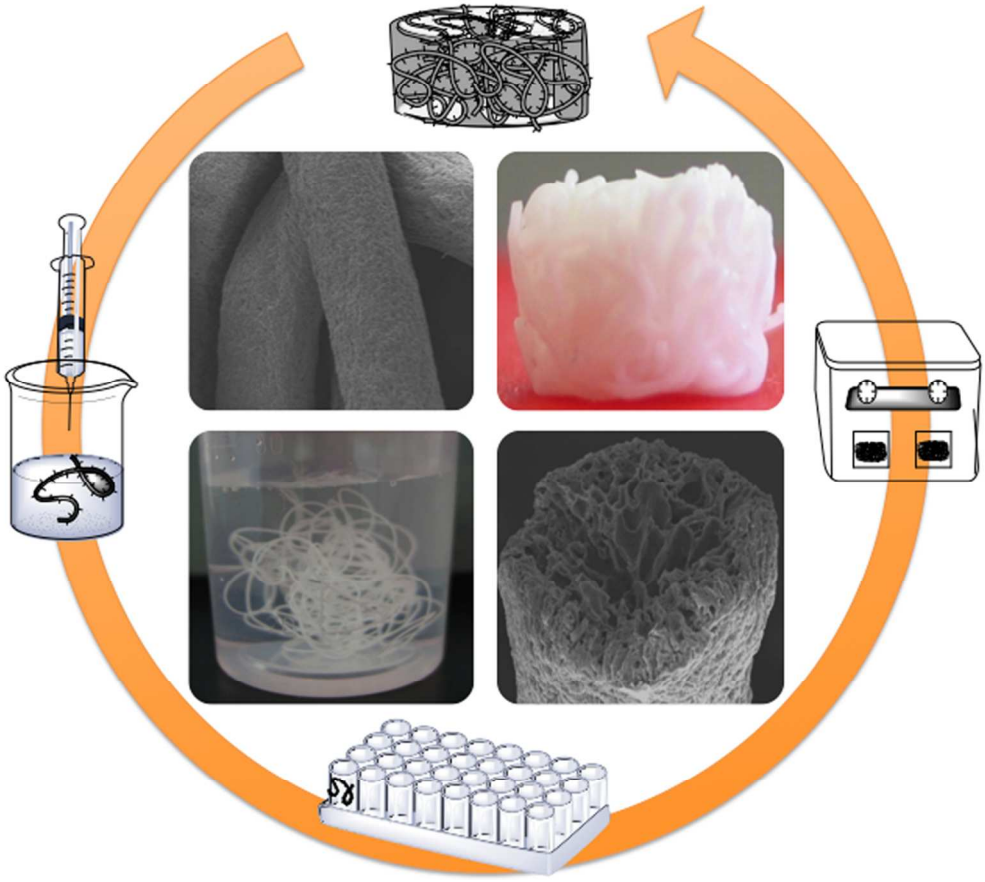

Elastic biodegradable fibre-mesh scaffolds for tissue engineering applications

Queen Mary University of London

Queen Mary, University of London
Mile End Road, London E1 4NS
Telephone: +44(0)20 7882 5555
Fax: +44 (0)20 7882 3390

School of Engineering & Materials Science
Dr Helena Azevedo
Senior Lecturer in Biomedical Engineering and Biomaterials
Direct Tel: +44(0)20 7882 5282
Email: h.azevedo@qmul.ac.uk

Dr Hilary J. Crichton, Associate Editor of Journal of Applied Polymer Science

Prof. Koon Gee Neoh, National University of Singapore, Guest Editor

January 20, 2014

Dear Dr Crichton and Prof. Neoh,

Thank you for the opportunity to reconsider our manuscript entitled "Elastic biodegradable starch/ethylene-co-vinyl alcohol fibre-mesh scaffolds for tissue engineering applications" (AP-2013-10-3525), for publication in the Journal of Applied Polymer Science, in particular in the Special Issue on Bioactive Surface Functionalization.

We have prepared a revised version with the changes requested by the reviewer. Please see below a detailed response (in *italics*) to all the concerns expressed by the reviewer and changes in the manuscript. The text modifications in the revised version are highlighted in yellow.
We hope these changes address any remaining concerns with this manuscript and you will find the manuscript worthy of publication in Journal of Applied Polymer Science

Thank you in advance for considering our manuscript and we look forward to hearing from you.
Yours sincerely,

Helena S. Azevedo

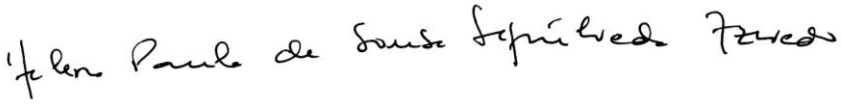

Response to Reviewer Comments and Text Modifications

Reviewer: 1

The authors present an interesting study on elastic biodegradable scaffolds for tissue regeneration application including scaffold manufacturing, morphological and mechanical characterisation, investigating the effect of in vitro degradation on scaffold morphology and mechanics and in vitro cell culture experiments. The study has been thoroughly conducted and the manuscript is well written. There are, however, some aspects of the manuscripts that need clarification.

We thank the reviewer for the valuable comments on our paper. Please see the answers to the raised questions and modifications in the text below.

1) Abstract: The statement that the degradation does not affect the elasticity of the scaffold is contradictory to the results and statement on p 17 that the scaffold mechanical properties were affected by the degradation. This needs clarification.

We agree with the reviewer's opinion on the contradictory statement in the abstract regarding the effect of degradation on the scaffold mechanical properties considering the results reported in pg 17. Therefore, we have removed the sentence from the abstract.

Methods:

2) The determination of interconnectivity from µCT data should be described in more detail.

We agree with the comment raised by the reviewer on the absence of details how the morphometric data was obtained and we have therefore included a more detailed description in the revised version. It is important to mention that all data for the morphometric analysis was obtained through the software of micro-CT, namely CT Analyser (v1.5.1.5 SkyScan) and ANT 3D creator (v2.4, SkyScan) for building the 3D virtual models. The mathematical models used in this software are not available (company secrecy). The revised version (M&M section) contains the following description to explain how we have obtained the morphometric data (porosity, pore size and interconnectivity).

"To assess the morphometric parameters (porosity, interconnectivity and pore size) of the scaffolds, the specimens were scanned in triplicate using a high-resolution µCT system (Skyscan 1072, Skyscan, Kontich, Belgium). The X-ray scans were acquired in high-resolution mode of 6.59 µm and an exposure time of 2.1 seconds. The energy parameters defined in the scanner were 69 keV with a current of 144 µA. Approximately 400 projections were acquired over a rotation range of 180◦ with a rotation step of 0.45◦. Datasets were reconstructed using standardized cone-beam reconstruction software (NRecon v1.4.3, SkyScan). The output format for each scaffold

was 400 serial bitmap images with 1024 × 1024 pixels. Representative dataset of 200 slides were segmented into binary images with a dynamic threshold of 37–120 (grey values). These data sets were used for morphometric analysis (CT Analyser v1.5.1.5, SkyScan) and to build the 3D virtual models (ANT 3D creator v2.4, SkyScan). The morphometric analysis was used to assess structural parameters for the scaffolds, which included porosity, interconnectivity and pore size. 3D virtual models of representative regions in the bulk of the scaffolds were created, visualized and registered using both images processing software (CT Analyser and ANT 3-D creator)."

3) Similarly, more details should be provided on how pore size was defined and determined.

The above description already includes the details that were also used on the determination of the pore size.

Data analysis of mechanical tests:

4) It would be interesting to know what compressive forces were measured in the context of the measurement error of the 1kN load cell used.

According with the manufacturer of the instrument (Instron), the 1kN load cell is reliable for compressive forces higher than 10 N (1% of the full load), with an accuracy of 0.25% of the indicated load. In all the tests the compressive modulus was measured for compressive forces higher than 10 N, which is within the operating range of the cell.

5) How linear or non-linear were the stress-strain curves for the scaffold samples?

The stress-strain curves for the scaffold samples had a linear region and the modulus was always determined by using a tangent to the initial linear portion of the load deformation curve. In the section material and methods of the original version, we have written the following sentence "in the cases that the yield stress was not clear it was calculated as the stress at the intersection of a line drawn parallel to the linear region and intercepting the x-axis at 1% strain". However, we have not reported the yield stress for the developed scaffolds in the manuscript. Because this might have generated some misunderstanding, we have removed the sentence from the text.

6) Was the linear region of the stress-strain curves used to calculate the modulus in the same strain region for different samples, i.e. was the modulus reported determined at the same or different strain for the various samples and groups?

The compressive modulus was always calculated in the initial linear region (strain < 1%) of the stress-strain curve for all samples. Although we have not indicated in the original version, a small preload was applied before testing the specimen in order to have the correct contact of the machine plates with the specimen, avoiding the occurrence of warping surface of the used specimens.

Results and Discussion:

7) Fibre thickness is given as one parameter to be determined from µCT data but has not been provided as a result. This should be included.

The fiber thickness was determined by SEM and not by µCT. We have clarified this point in the revised manuscript (section "Morphological and mechanical characterization of fibre-mesh scaffolds: Scanning electron microscopy (SEM)") and included the estimated value (215 µm) in the text.

8) p 11: It is stated that the porosity values measured might be considered low for bone tissue engineering. This is however not further discussed but should be done.

As recommended, we have included further discussion on the appropriateness of the porosity values as follows:

"Although the values for porosity might be considered low when compared with the ones reported as optimal for bone regeneration, other factors should be considered when designing the scaffold porosity, like the degradation rate of the scaffold and the intended application. Porosity is expected to increase with degradation and high porosity may constrain the mechanical strength of the scaffold which may be critical for the regeneration of load-bearing tissues such as bone."

We hope the added text addresses the reviewer's request.

9) On page 12, the internal porous structure of SEVA-C fibres is mentioned. Do porosity and pore size results for the scaffold include this internal fibre porosity? It is also stated that the internal porosity will contribute to the increase of cell anchorage sites. Wouldn't this require a porosity of the fibre surface to provide access routes to the inner structure of the fibres? This should be clarified/discussed.

The porosity and pore size was determined by µCT and the internal porosity of the fibers was not taken into account for the porosity results. We agree with the reviewer's comment on the irrelevance of the internal porosity for cell attachment. The internal porosity can be beneficial for the loading of drugs for stimulating attached cells, but not for cell adhesion. Therefore, we have removed that sentence from the text.

Minor comments

Fig 1: Text labels are illegible

We have increased the size of labels in Fig 1.

Fig 2: Text label at scale bar is illegible in insert of fig (c) Fig 3: Text labels are difficult to read Fig 5 c and d: Text labels are either difficult to read or illegible Fig 6: The graph indicates showing compressive stress whereas the caption refers to compressive modulus. This needs to be clarified.

We have increased the size of the text in all Figures. We thank the reviewer for the observation on the title of the graph axis of Fig. 6 and we have corrected it.

Table 1 should be omitted as data is already presented in the results (p 13 bottom)

As suggested, we have removed Table 1 from the manuscript.

Elastic biodegradable starch/ethylene-co-vinyl alcohol fibre-mesh scaffolds for tissue engineering applications

Maria A. Susano[1,2], Isabel B. Leonor[1,2], Rui L. Reis[1,2], Helena S. Azevedo[1,2]

[1]3B's Research Group - Biomaterials, Biodegradables and Biomimetics, University of Minho, Headquarters of the European Institute of Excellence on Tissue Engineering and Regenerative Medicine, AvePark, 4806-909 Taipas, Guimarães, Portugal

[2]ICVS/3Bs - PT Government Associate Laboratory, Braga/Guimarães - Portugal

Correspondence to: Helena S. Azevedo. Present address: School of Engineering&Materials Science, Queen Mary University of London, Mile End, E1 4NS, London, UK. E-mail: hazevedo@dep.uminho.pt; h.azevedo@qmul.ac.uk

ABSTRACT

The fabrication of a biomaterial scaffold, with adequate physical and structural properties for tissue engineering applications, is reported. A blend of starch with ethylene-vinyl alcohol (50:50% w/w, SEVA-C) is used to produce 3D fibre-mesh scaffolds by wet-spinning. The scaffolds are characterized in terms of morphology, porosity, interconnectivity and pore size, using scanning electron microscopy (SEM) and micro-computed tomography (μCT). The degradation behaviour, as well as the mechanical properties of the scaffolds, is investigated in presence of alpha-amylase enzyme at physiological concentration. Scaffolds with porosities ranging from 43% to 52%, interconnectivity of approximately 70.5% and pore size between 118 μm and 159 μm, can

be fabricated using the proposed methodology. The scaffolds exhibit an elastic behaviour in the wet state with a compressive modulus of 7.96 ± 0.32 MPa. Degradation studies show that SEVA-C scaffolds are susceptible to enzymatic degradation by alpha-amylase, confirmed by the increase of weight loss (40% of weight loss after 12 weeks) and presence of degradation products (reducing sugars) in solution. The diameter of SEVA-C scaffolds decreases with degradation time, increasing the overall porosity, interconnectivity and pore size. In vitro cell studies with human osteosarcoma cell line (SaOs-2) showed a nontoxic and cytocompatible behaviour of the developed fibre mesh scaffolds. The positive cellular response, together with structural and degradable properties, suggests that 3D SEVA-C fibre-meshes may be good candidates as tissue engineering scaffolds.

KEYWORDS

Starch-blend; wet-spinning; fibre-mesh scaffold; degradation behaviour; elastic properties; tissue engineering.

INTRODUCTION

Tissue engineering often makes use of biodegradable scaffolds to guide and promote controlled cellular growth and differentiation in order to generate new tissue. Over the past decades, a variety of scaffolds, made of natural[1] and synthetic[2-3] polymer-based materials and fabricated by different methods,[4-7] have been investigated and significant research has been carried out studying the effects of scaffold structural and mechanical properties on tissue formation. Within different tissues, elasticity spans almost three orders of magnitude across brain, fat, muscle, cartilage and bone.[8] Elasticity is one intrinsic physical property that is well controlled in many tissues and it is well recognized that cells sense the elasticity of their microenvironments. Therefore, major efforts have been taken to develop elastomeric biomaterials that mimic the elastic behaviour of native tissues. Elastomeric biomaterials include chemically crosslinked (silicones, polyolefin and polydiene, poly(polyol sebacate, cis-poly(isoprene)) and physically crosslinked (polyurethanes, styrene-based rubbers, polyesters and copolyesters) elastomers.[9] Each type of material has its advantages and disadvantages, in terms of biocompatibility, biodegradability and mechanical properties. A recent review on the use of elastomeric biomaterials for tissue engineering revealed that ideal elastomeric materials with optimal properties are still not available for clinical applications.[9]

In the recapitulation of cellular microenvironments, scaffolds may play an important role in providing a platform to influence the perception and response of cells to substrate mechanics. In the last years, several studies have demonstrated that the function of cells, in particular stem cells, is affected by collective physical properties (elasticity, topography, and geometry) of materials. [8,10-12] It is believed that matrix stiffness may regulate cell function by altering cell

shape, resulting in cytoskeletal rearrangements and altered signalling. The results suggest the possibility of optimizing matrix elasticity to control cell behaviour and foster regeneration.

Our group has reported the preparation of fibres by wet-spinning using a blend of starch with poly-(ethylene-vinyl alcohol) copolymer (SEVA-C)[13] and shown that the obtained wet spun fibres presented some interesting features when compared with melt spun fibres using the same polymeric blend.[14] Thinner and much stiffer fibres can be produced and their rough surface may favour cell adhesion. In this paper, the fabrication of 3D fibre-mesh scaffolds using the SEVA-C blend and a nondesigned-controlled technique is described. Their structural, mechanical and degradation characteristics are reported as well as their ability to support cell survival and proliferation.

EXPERIMENTAL

Fabrication of 3D fibre-mesh scaffolds

The scaffolds investigated in this study were fabricated by wet-spinning technique (Figure 1) and using a commercial blend of starch with poly-(ethylene-vinyl alcohol) copolymer (SEVA-C, 50:50 wt%) provided by Novamont (Mater Bi 1128RR, Novara, Italy). SEVA-C granules were dissolved in dimethyl sulfoxide (DMSO, Riedel-de Haën). The obtained polymer solution (20%, w/v) was loaded into a syringe (12.5 mm diameter, 25G needle) which was placed in a programmable syringe pump (World Precision Instruments, UK). The polymer solution (0.5 mL) was injected at controlled rate (0.2 mL/h) directly into a water bath to allow the formation of the fibres (Figure 2-a). The fibres were washed several times with distilled water to remove residual DMSO. To ensure reproducibility, fibre-mesh scaffolds were prepared by placing a

predetermined volume of fibres in a well of a 48-well cell culture plate. The fibres were dehydrated with increasing concentrations of ethanol (50, 60, 70, 80, 85, 90, 95 and 100%) and then allowed to dry at room temperature. To ensure the bonding between the fibres, the scaffolds were put in the oven for 15 min at 160 ºC, as shown in Figure 1. For cell culture studies, the scaffolds were sterilized by ethylene oxide, with a cycle time of 14 h at a working temperature of 45 ºC and a chamber pressure of 50 kPa, conditions previously optimised for the SEVA-C blend.[15]

Morphological and mechanical characterization of fibre-mesh scaffolds

Scanning electron microscopy (SEM)

To observe the structure and morphology of the fibre-mesh scaffolds, the samples were mounted onto aluminium stubs with a carbon tape and gold sputter-coated (Fisons Instruments, Sputter Coater SC502, UK). Microphotographs at the surface were collected with a Leica Cambridge S-360 model (Cambridge, UK) scanning electron microscope. The fibre thickness was estimated by measuring the thickness of individual fibres obtained in the SEM images.

Micro-computed tomography (µCT)

To assess the morphometric parameters (porosity, interconnectivity and pore size) of the scaffolds, the specimens were scanned in triplicate using a high-resolution µCT system (Skyscan 1072, Skyscan, Kontich, Belgium). The X-ray scans were acquired in high-resolution mode of 6.59 µm and an exposure time of 2.1 seconds. The energy parameters defined in the scanner were 69 keV with a current of 144 µA. Approximately 400 projections were acquired over a rotation range of 180◦ with a rotation step of 0.45◦. Datasets were reconstructed using standardized cone-beam reconstruction software (NRecon v1.4.3, SkyScan). The output format

for each scaffold was 400 serial bitmap images with 1024 × 1024 pixels. Representative dataset of 200 slides were segmented into binary images with a dynamic threshold of 37–120 (grey values). These data sets were used for morphometric analysis (CT Analyser v1.5.1.5, SkyScan) and to build the 3D virtual models (ANT 3D creator v2.4, SkyScan). 3D virtual models of representative regions in the bulk of the scaffolds were created, visualized and registered using both images processing software (CT Analyser and ANT 3-D creator).

Mechanical testing

Compression tests were carried out to evaluate mechanical behaviour of the scaffolds in the dry and wet state (scaffolds immersed in PBS for 24 hours). Seven specimens with height ~ 3 mm and diameter ~ 7 mm were tested for each condition. They were tested using uniaxial testing system (Instron 5540 Universal Machine, USA) with a load cell of 1 kN. Compression testing was carried out at a crosshead speed of 2 mm/min, until obtaining a maximum reduction in samples height of 60%. The compressive modulus was determined in the most linear region (strain < 1%) of the stress-strain graph.

Scaffold degradation

The degradation of the scaffolds was assessed in absence and presence of α-amylase enzyme to study its effect on starch hydrolysis. Pre-weighed fibre-mesh scaffolds (previously dried under vacuum at 60 ºC for 48 h) were individually immersed in 2 mL of phosphate-buffered saline (PBS, 0.01 M, pH 7.4) solution containing 160 U/L α-amylase (EC 3.2.1.1, from *Bacillus* sp., Sigma) and incubated for 1, 4, 8 and 12 weeks at 37 ºC. Sodium azide (0.02%) was added to the buffer solution to prevent microbial growth. The degradation solutions were changed weekly. A control, in PBS only, was also performed and five samples were analysed for each condition.

After each degradation period, the samples were removed from the solution and placed between two filter papers, to remove excess of liquid, immediately weighed, washed several times with distilled water and placed in the vacuum oven at 60 ºC for 48 h in order to determine water uptake and weight loss. The degraded scaffolds were also analysed by SEM, µCT and the mechanical properties were evaluated in the wet state, as described above. Degradation solutions (collected every week) were analysed to determine the concentration of reducing sugars released into the solution as result of starch hydrolysis. The determination of reducing sugars in solution was based on the dinitrosalicyclic acid (DNS) method.[16] Absorbance was read at 540 nm in a microplate reader (Synergy HT, BIO-TEK Instruments, USA) using a standard curve of glucose. The concentration of reducing sugars at each degradation time was calculated as cumulative values obtained from the weekly determinations.

Cell culture studies

To investigate if the SEVA-C scaffolds can support cell viability and proliferation, an established human osteosarcoma cell line (SaOs-2) obtained from European Collection of Cell Cultures (ECACC, UK) was used. Cells cultured onto tissue culture polystyrene (TCPS) with standard culture medium were used as a negative control. Prior cell seeding, cells were cultured in DMEM (Dulbecco's-Modified Eagle's Medium, Sigma, Germany) supplemented with 10% fetal bovine serum (Gibco, UK), 1% antibiotic-antimycotic (Gibco, UK) solution containing 10,000 units/mL penicillin G sodium, 10,000 µg/mL streptomycin sulphate and 25 µg/mL amphotericin B as Fungizone® in 0.85% saline in a humidified atmosphere with 5% CO_2 and at 37 ºC. When confluence was reached, cells were trypsinized (0.25% trypsin/EDTA solution, Sigma Chemical, USA) from the culture flask and diluted to achieve a cellular concentration of 26,000 cells/mL.

Afterwards, 50 µL of a cell suspension was dropped onto the 3D scaffolds, individually placed in each well of a 48-well cell culture plate, and incubated for 4 h in 5% CO_2 incubator at 37 ºC. Subsequently, 500 µL of DMEM were added to the wells and further incubated for 1, 3, 7 and 14 days in the same conditions. The culture medium was changed every two days. Viability of cells was assessed by the MTS assay and cell proliferation evaluated by DNA quantification, as described below.

Cell viability

Cell viability was determined by means of a standard MTS (3-(4,5-dimethylthiazol-2-yl)-5-(3-carboxymethoxyphenyl)-2-(4-sulfophenyl)-2H-tetrazolium) assay. The MTS test was performed according to the manufacturer's instructions (CellTiter 96 One Solution Proliferation Assay Kit, Promega, USA). Briefly, the cell cultured scaffolds were treated with 200 µL/well of MTS reagent solution in serum-free DMEM without phenol red (5:1 ratio) and incubated for 3 hours at 37 ºC in a humidified environment containing 5% of CO_2. 100 µL of medium from each well were transferred to a 96-well plate and the absorbance at 490 nm was determined in the microplate reader (Synergy HT, BioTek Instruments, USA). The absorbance of each sample from three independent assays was measured in triplicate. Unseeded scaffolds were used as controls.

Cell proliferation

Cell proliferation was evaluated by quantifying the DNA amount of the cells in the scaffolds at different time points using PicoGreen® DNA quantification assay (Molecular Probes, USA). The DNA of cultured cells was extracted by osmotic lysis and thermal shock. Cell cultured scaffolds were collected, washed twice with sterile PBS (Sigma, USA) solution and transferred into 1.5 mL tubes containing 1 mL of ultra-pure water. Scaffolds, with or without cells, were stored at -80

ºC. Samples were thawed and the supernatant was collected for DNA quantification following the manufacturer's instructions. The fluorescence was measured (485 nm excitation and 528 nm emission) in a microplate reader (Synergy HT, BioTek Instruments, USA). The DNA amounts were calculated from a calibration curve of DNA standards. Each sample was analyzed in triplicate.

Statistical analysis

All data are given as mean ± standard deviation (SD) for n = 5 (degradation), n = 7 (mechanical testing) and n = 3 (µCT and *vitro* cell culture experiments). Normality test, Shapiro-Wilk, was performed to insure data set is well-modelled by a normal distribution. A statistical hypothesis test using a Student's *t* distribution (two samples t-test) was used to identify differences in the results. The data analyses were performed with OriginPro software (version 8) and differences were considered significant at $p < 0.05$.

RESULTS AND DISCUSSION

Morphological characterization

In scaffold-based tissue engineering, scaffold architectural features should be designed to allow the diffusion of nutrients and cell migration and thus promoting optimal tissue ingrowth *in vivo*. Some of these important architectural characteristics include porosity, pore size and interconnectivity. In the present study, SEVA-C fibres were produced by wet-spinning (Figure 2a) and moulded into a cylindrical shape (Figure 2b). To maintain the fibres within the mesh when immersed in aqueous solutions, the obtained scaffolds were further submitted to a heat treatment for binding the fibres. µCT and SEM were used to assess the relevant morphometric

parameters of the scaffolds. SEM images show fibres with an average thickness of 215 µm and rough surface (Figure 2c,d) which may provide favourable anchorage sites for cell attachment. Representative 3D images of the scaffolds by µCT reveal a fibre mesh structure with a random distribution of the fibres within the mesh and a good level of interconnectivity (Figure 2e-f). This type of scaffold provides a highly permeable, interconnected structure with a large surface area. The SEVA-C scaffolds have a pore volume fraction of 47.3% ± 5.16% with an interconnectivity of 70.5% ± 4.12%, as determined by µCT analysis. Porosity is a key property since it determines cell seeding efficiency, diffusion and the mechanical strength of the scaffold. When molecular transport is hampered, due to poor diffusion, cell-scaffold constructs exhibit peripheral cellular growth while the interior of the construct undergoes necrosis.[17] In addition, high porosity (up 90%) is recommended to enhance cellular attachment and neo-tissue ingrowth under *in vivo* conditions.[2,18,19] Although the values for porosity might be considered low when compared with the ones reported as optimal for bone regeneration, other factors should be considered when designing the scaffold porosity, like the degradation rate of the scaffold and the intended application. Porosity is expected to increase with degradation[19] and high porosity may constrain the mechanical strength[6] of the scaffold which may be critical for the regeneration of load-bearing tissues such as bone.

The functionality of tissue engineering scaffolds is also related with the size of the pores. An exact pore size cannot be suggested as a general guide for optimal tissue outcomes, due to the specificity of each tissue to be engineered. Relatively larger pores favour direct tissue regeneration since they allow vascularisation and high oxygenation. Specifically, in bone tissue engineering, the consensus seems to be that the optimal pore size for bone ingrowths is 100-

400 µm.[20-22] However, more recently, studies have shown that 3D structures containing microporosity (< 10 µm) as well as macroporosity (> 50 µm), a multi-scale porosity, can further promote bone ingrowth.[23-24] Conversely, scaffolds that contained only macroporosity, and no microporosity, had no bone ingrowth.[24] The developed scaffold shows a mean pore size of 138.9 µm ± 20.37 µm and pore distribution with sizes between 30-280 µm (data not shown), in the range of the optimal pore size for bone ingrowth and simultaneously for a fast osseointegration. The distribution of fibres within the mesh influences the pore size, which can be controlled by the amount of fibres used for the scaffold production and also by the degree of compaction of the fibres.

Most polymeric fibres described in the literature and obtained from other processing techniques exhibit a very dense core.[14,25-26] In contrast, the SEVA-C fibres show an internal porous structure, as observed in the SEM micrographs of the fibre cross-section (Figure 2d). We anticipate that this internal porosity may be a beneficial attribute for the incorporation and sustained release of differentiation agents relevant in tissue engineering applications.

The nondesigned-controlled technique used in this study allows attaining some control over the 3D architecture, in terms of porosity and pore size, by altering some processing parameters, such as fibre diameter and volume of fibres. However, one has to consider that there is a compromise between porosity and mechanical behaviour. An increase in the void volume results in a reduction in the mechanical strength of the scaffold, which can be critical for tissue regeneration. On the other hand, a highly porous scaffold may not have interconnected pores, thus lowering the diffusion efficiency.[27] Studies performed by Suh *et al*. showed superior cell attachment and proliferation of chondrocytes in scaffolds with high interconnectivity and equal

porosity.[28] Lu *et al*. also reported the importance of interconnectivity for bone ingrowth.[29] Thus, a high interconnected structure, such as the one propose herein, is essential to allow the diffusion of culture medium, metabolic waste and oxygen, and to facilitate the infiltration and proliferation of cells.[30]

Mechanical characterization

The magnitudes of mechanical stresses that tissues may be subjected *in vivo* can be quite large, and few engineered tissue constructs possess the properties to withstand such stresses at the time of implantation. The challenge is not only matching a single mechanical parameter of the tissue to be engineered, such as modulus or strength, but one needs to consider that most tissues possess complex viscoelastic, non linear, and anisotropic mechanical properties that may vary with age, site, and some other factors. The maintenance of the scaffold structural integrity is important for achieving stable biomechanical conditions at the host site.[31] Additionally, in the case of load-bearing tissue, such as cartilage and bone, the scaffold matrix must provide sufficient mechanical support to withstand *in vivo* stress and loading.[6] There are a couple of important considerations regarding the scaffold properties for hard tissues. As pointed by Cordell *et al.*,[32] one must consider that the stiffness of the scaffolds would increase with tissue ingrowth, especially in slowly degrading materials. Although the mechanical properties of bone depends on its structure and orientation, the values of compressive modulus of normal wet human cancellous bone reported in the literature vary between 12 and 900 MPa[33]. While many studies report the mechanical properties of scaffolds in the dry state, assessing their mechanical behaviour in the hydrated sate is physiologically more relevant. As expected, the results of mechanical testing demonstrate that the values of compressive

modulus for SEVA-C scaffolds are clearly different in the dry and wet state. In the dry state, the SEVA-C scaffolds exhibited a compressive modulus (E) of 24.31 ± 2.91 MPa, while in the wet state the compressive elastic modulus is reduced to 7.96 ± 0.32 MPa. One explanation in the decrease of the modulus after immersion in PBS can be attributed to the plasticization effect due to the absorbed water. SEVA-C is a very hydrophilic material and after being in contact with aqueous solutions absorbs water, becoming more flexible that result in a decrease of compressive modulus. Although these values are considered below the ones required for bone applications, SEVA-C scaffolds present higher compressive modulus than other fibre-mesh scaffolds obtained from blends of starch with biodegradable polyesters (polycaprolactone and poly(lactic acid)).[34] The mechanical properties of the developed scaffolds can be enhanced by coating the SEVA-C fibres with calcium-phosphate layer. Interestingly, the mechanical characterization of SEVA-C scaffolds in the wet state showed that after compression, SEVA-C fibre mesh scaffolds present an elastic behaviour since they recover almost completely their original dimensions within 24 hours (Figure 3). This indicates a remarkable ability to withstand firm thumb pressure without permanent deformation. On the contrary, in the dry state, the deformation consequence of compression load is permanent. In addition, hydrated SEVA-C scaffolds possess adequate compressive modulus to support their shape without structure collapse and thereby maintaining pore structure in 3D. The elastic behaviour of the scaffold represents an important advantage since the scaffolds can be subjected to mechanical stimuli during cell culture without being permanently deformed as mechanical forces are believed to affect cellular distribution,[35] metabolic activity[36] and ultimately the mechanical properties of

the tissue itself.[37] Therefore, the 3D structures proposed herein show a good combination of morphometric parameters and mechanical performance.

Degradation behaviour

Under physiological conditions, biodegradable polymers are mainly degraded by hydrolysis followed by oxidation. There are two different mechanisms for hydrolysis: polymers that are decomposed by enzyme-specific reactions (enzymatically degradable polymers) and polymers that are decomposed by contact with water or serum. α-Amylase is a glycosidic hydrolase that acts on the α (1-4) glycosidic bonds of starch molecules reducing its molecular weight, and yielding maltose, glucose and other small sugar molecules. In humans, the enzyme occurs in a variety of tissues, but the highest concentrations are in the pancreas and in salivary glands. Low amylase activities are normally detected in the serum (46-244 U/L) of healthy subjects.[38] Having into account the catalytic activity of α-amylase, the degradation behavior of SEVA-C scaffolds was studied in presence of this enzyme at a physiological concentration (160 U/L). Degradation was assessed by following the scaffold weight loss and water uptake along the time (Figure 4). The concentration of reducing sugars in solution was also determined since it can be used to estimate the degradation of polysaccharide materials. Polysaccharide that are reducing sugars, generally have only one residue that lacks a glycosidic linkage, the so-called reducing end. When consecutively hydrolysis of glycosidic linkages occurs, there is the release of soluble reducing sugars into the solution, which can be quantified.

The scaffolds kept in PBS, devoid of enzymes, showed lower degradation rate (< 10% weight loss after 12 weeks of incubation) comparing with ones in amylase solution (~ 40% weight loss). The low percentage of weight loss in PBS reveals the stability of the scaffolds in buffer solutions.

Moreover, the fibre mesh scaffolds had enough mechanical integrity to remain intact throughout the water uptake and degradation study. Previous studies have already demonstrated the biodegradable character of SEVA-C materials[39] but these studies were performed on compact samples processed by injection moulding. The presence of starch increases the biodegradability of the blend making it susceptible to enzyme degradation by α-amylase. As the degradation time increases, an accentuated increase in the concentration of sugars in solution is observed confirming the degradation of starch in the scaffold. The concentration of sugars in solution when the scaffold was incubated in the enzyme solution (8 $mg.mL^{-1}$) is about 5 times higher that the value found in PBS only (1.8 $mg.mL^{-1}$) at 12 weeks. Water uptake was also investigated along degradation time (Figure 4b). When immersed in PBS, the water up-take is about 120% after one week and remains constant with time. The high values of water uptake are related with the hydrophilic nature of the SEVA-C material (presence of -OH groups in starch and EVOH) and also with the high surface area of the fibre mesh scaffold. In the enzymatic solution, higher water uptake was observed in the first week (~ 200%) which increases gradually with time of degradation. The enhanced permeability of the material over time, caused by enzymatic degradation, leads to increased water absorption.

To assess the effect of degradation on the scaffold 3D structure, μCT and SEM analyses were performed (Figure 5). Changes in the scaffold structure at the surface level were detected, being more visible after 12 weeks of degradation, where a rougher surface is observed (Figure 5b). The morphological changes, porosity and interconnectivity during degradation were examined by μCT. The results of the morphological analysis (Figure 5c-d) show an increase in the interconnectivity for the scaffolds immersed in the enzymatic solution, about 17%, while for

the samples immersed in PBS the increase was not so notorious (approximately 5%). In terms of porosity, a similar trend was observed with an increase in the void volume of the scaffolds with degradation time. The porosities of scaffolds in PBS and enzymatic solution after 12 weeks are 71% and 75%, respectively (Figure 5d, an increase of almost 30% related with initial porosity). Surface morphology is also affected during scaffold degradation. The scaffolds immersed in amylase solution present notorious changes on the surface morphology, whereas the scaffolds immersed in PBS did not show evident surface alterations (Figure 5b). After 4 weeks of degradation, there is a noticeable increase on surface roughness, being this observation more pronounced after 12 weeks. Moreover, a decrease in the diameter of the scaffolds was also observed after degradation (Figure 5a). The removal of starch component by enzyme hydrolytic activity leads to the partial matrix collapse[40] culminating in a reduction of the scaffold size. This is a very important aspect considering that the degradation profile of a scaffold material should leave enough space for new tissue ingrowth.[34]

Since the mechanical properties affect scaffold functionality, the compressive modulus of the scaffolds was determined along the degradation time. As expected, the scaffold mechanical properties are affected by the scaffold degradation (Figure 6). The decrease in the compressive modulus is associated with increased porosity observed along degradation. The lower values in compressive modulus are more pronounced for the scaffolds immersed in the enzymatic solution, in which a reduction of about 75% was observed after 12 weeks of degradation. For the scaffolds immersed in PBS only, the compressive modulus was approximately 4 MPa after 12 weeks.

Cellular viability and proliferation

To consider the use of the scaffolds in tissue engineering, the biocompatibility of the scaffolds in regards to cell viability and proliferation was evaluated. The viability of the cells seeded on the developed scaffolds is shown in Figure 7a. MTS assay (Figure 7a) proved that cells remain viable, as observed by an increased metabolic activity with culturing time, indicating that the scaffolds did not have any toxic effect on the cells. DNA quantification was also performed to evaluate cell proliferation (Figure 7b). With the progress of culture period, a significant increase in DNA amount was observed, indicating an increase in cell proliferation. Although for initial times (until 7 days) the amount of quantified DNA was lower, the initial *in vitro* performance of scaffold materials is determined by the intrinsic properties of the 3D structure when the first occurring events are related with cell-biomaterial interaction. At later stages, other factors, such as cell to cell contact, are expected to play a significant role. These results indicate that the developed scaffolds may be adequate for the growth of other cell types (stem cells) and future studies will be performed to evaluate cell attachment, proliferation and differentiation of mesenchymal stem cells on these fibre-mesh scaffolds.

CONCLUSIONS

3D fibre-mesh scaffolds made of a blend of starch with poly-(ethylene-vinyl alcohol) copolymer were successfully prepared by wet-spinning. The scaffolds showed interesting properties, including a structure with high porosity and surface area for cell attachment and infiltration; susceptibility to enzymatic degradation (40% of weight loss after 12 weeks) keeping adequate structure for tissue ingrowth; and elastic behaviour in the wet state (the scaffolds are able to rapidly recover the initial structure after compression), which represents an additional

advantage when compared with existing scaffold materials. Moreover, *in vitro* studies showed that the developed scaffolds support cell viability and proliferation. The positive cellular response, together with structural and degradable properties, suggests that 3D SEVA-C fibre-meshes may be good candidates as tissue engineering scaffolds.

ACKNOWLEDGEMENTS

This work was supported by national funds through the Portuguese Foundation for Science and Technology under the scope of the project PTDC/CTM/67560/2006 and by the European Regional Development Fund (ERDF) through the Operational Competitiveness Programme "COMPETE" (FCOMP-01-0124-FEDER-007148). We thank Dr Emanuel Fernandes of the 3B's Research Group at the University of Minho for his assistance analyzing the data from mechanical tests.

REFERENCES

1. J. F. Mano, G. A. Silva, H. S. Azevedo, P. B. Malafaya, R. A. Sousa, S. S. Silva, L. F. Boesel, J. M. Oliveira, T. C. Santos, A. P. Marques, N. M. Neves, R. L. Reis, *Journal of the Royal Society Interface*, **4**, 999-1030 (2007).
2. L. E. Freed, G. Vunjaknovakovic, R. J. Biron, D. B. Eagles, D. C. Lesnoy, S. K. Barlow, R. Langer, *Bio-Technology*, **12**, 689-693 (1994).
3. M. Martina, D. W. Hutmacher, *Polymer International*, **56**, 145-157 (2007).
4. T. Weigel, G. Schinkel, A. Lendlein, *Expert Review of Medical Devices*, **3**, 835-851 (2006).
5. C. Liu, Z. Xia, J. T. Czernuszka, *Chemical Engineering Research & Design*, **85**, 1051-1064 (2007).
6. S. J. Hollister, *Nature Materials*, **4**, 518-524 (2005).
7. S. J. Hollister, *Advanced Materials*, **21**, 3330-3342 (2009).
8. A. J. Engler, S. Sen, H. L. Sweeney, D. E. Discher, *Cell*, **126**, 677-689 (2006).
9. Q. Z. Chen, S. L. Liang, G. A. Thouas, *Progress in Polymer Science*, **38**, 584-671 (2013).
10. D. E. Discher, P. Janmey, Y. L. Wang, *Science*, **310**, 1139-1143 (2005).
11. W. E. Thomas, D. E. Discher, V. P. Shastri, *Mrs Bulletin*, **35**, 578-583 (2010).
12. P. M. Gilbert, K. L. Havenstrite, K. E. G. Magnusson, A. Sacco, N. A. Leonardi, P. Kraft, N. K. Nguyen, S. Thrun, M. P. Lutolf, H. M. Blau, *Science*, **329**, 1078-1081 (2010).
13. I. Pashkuleva, P. M. Lopez-Perez, H. S. Azevedo, R. L. Reis, *Materials Science & Engineering C-Materials for Biological Applications*, **30**, 981-989 (2010).
14. M. P. Pavlov, J. F. Mano, N. M. Neves, R. L. Reis, *Macromolecular Bioscience*, **4**, 776-784 (2004).
15. R. L. Reis, S. C. Mendes, A. M. Cunha, M. J. Bevis, *Polymer International*, **43**, 347-352 (1997).
16. T. K. Ghose, *Pure and Applied Chemistry*, **59**, 257-268 (1987).
17. S. L. Ishaug, G. M. Crane, M. J. Miller, A. W. Yasko, M. J. Yaszemski, A. G. Mikos, *Journal of Biomedical Materials Research*, **36**, 17-28 (1997).
18. B. S. Kim, D. J. Mooney, *Trends in Biotechnology*, **16**, 224-230 (1998).
19. V. Karageorgiou, D. Kaplan, *Biomaterials*, **26**, 5474-5491 (2005).
20. J. D. Bobyn, R. M. Pilliar, H. U. Cameron, G. C. Weatherly, *Clinical Orthopaedics and Related Research*, 263-270 (1980).
21. B. Otsuki, M. Takemoto, S. Fujibayashi, M. Neo, T. Kokubo, T. Nakamura, *Biomaterials*, **27**, 5892-5900 (2006).
22. M. Mastrogiacomo, S. Scaglione, R. Martinetti, L. Dolcini, F. Beltrame, R. Cancedda, R. Quarto, *Biomaterials*, **27**, 3230-3237 (2006).
23. J. G. Dellinger, J. A. C. Eurell, R. D. Jamison, *Journal of Biomedical Materials Research Part A*, **79A**, 223-U224 (2006).
24. J. R. Woodard, A. J. Hilldore, S. K. Lan, C. J. Park, A. W. Morgan, J. A. C. Eurell, S. G. Clark, M. B. Wheeler, R. D. Jamison, A. J. W. Johnson, *Biomaterials*, **28**, 45-54 (2007).
25. S. Chung, M. P. Gamcsik, M. W. King, *Biomedical Materials*, **6**(2011).
26. V. M. Correlo, A. R. Costa-Pinto, P. Sol, J. A. Covas, M. Bhattacharya, N. M. Neves, R. L. Reis, *Macromolecular Bioscience*, **10**, 1495-1504 (2010).
27. S. T. Ho, D. W. Hutmacher, *Biomaterials*, **27**, 1362-1376 (2006).
28. S. W. Suh, J. Y. Shin, J. H. Kim, J. G. Kim, C. H. Beak, D. I. Kim, S. J. Kim, S. S. Jeon, I. W. Choo, *Asaio Journal*, **48**, 460-464 (2002).
29. J. X. Lu, B. Flautre, K. Anselme, P. Hardouin, A. Gallur, M. Descamps, B. Thierry, *Journal of Materials Science-Materials in Medicine*, **10**, 111-120 (1999).
30. F. J. O'Brien, B. A. Harley, I. V. Yannas, L. J. Gibson, *Biomaterials*, **26**, 433-441 (2005).
31. P. B. Malafaya, T. C. Santos, M. van Griensven, R. L. Reis, *Biomaterials*, **29**, 3914-3926 (2008).

32. J. M. Cordell, M. L. Vogl, A. J. W. Johnson, *Journal of the Mechanical Behavior of Biomedical Materials*, **2**, 560-570 (2009).
33. K. A. Athanasiou, C. F. Zhu, D. R. Lanctot, C. M. Agrawal, X. Wang, *Tissue Engineering*, **6**, 361-381 (2000).
34. M. E. Gomes, H. S. Azevedo, A. R. Moreira, V. Ella, M. Kellomaki, R. L. Reis, *Journal of Tissue Engineering and Regenerative Medicine*, **2**, 243-252 (2008).
35. P. S. Eggli, E. B. Hunziker, R. K. Schenk, *Anatomical Record*, **222**, 217-227 (1988).
36. B. Vanwanseele, E. Lucchinetti, E. Stussi, *Osteoarthritis and Cartilage*, **10**, 408-419 (2002).
37. A. C. Swann, B. B. Seedhom, *British Journal of Rheumatology*, **32**, 16-25 (1993).
38. L. Isenman, C. Liebowand S. Rothman, *American Journal of Physiology-Endocrinology and Metabolism*, **276**, E223-E232 (1999).
39. H. S. Azevedo, F. M. Gama, R. L. Reis, *Biomacromolecules*, **4**, 1703-1712 (2003).
40. H. S. Azevedo, R. L. Reis, *Acta Biomaterialia*, **5**, 3021-3030 (2009).

FIGURE 1 Schematic illustration of the setup for the production of the fibre-mesh scaffolds using wet-spinning technique.

FIGURE 2 SEVA-C fibres after processing by wet-spinning **(a)** and after moulding into a 3D structure **(b)**. SEM images of SEVA-C fibre mesh scaffolds **(c)** and fibre cross-section **(d)**. Inset in **(c)** is lower magnification of SEM image. 2D **(e)** and 3D **(f)** visualizations obtained by μCT analysis.

FIGURE 3 Scaffold dimensions in terms of height and diameter (Ø) before and after compression test (load cell of 1 kN; crosshead speed 2 mm/min; 60% strain).

FIGURE 4 Degradation profile of the SEVA-C fibre-mesh scaffolds measured in terms of **(a)** weight loss (----) and reducing sugar concentrati□( ) and **(b)** water uptake as function of degradation time in PBS solution (pH 7.4, 37 ºC) and in presence of α-amylase. A single asterisk (*) indicates a significant difference (p<0.05) for the same sample at different time points. A plus (+) indicates a significant difference (p<0.05) between conditions for the same time point.

FIGURE 5 μCT **(a)** and SEM **(b)** images of SEVA-C fibre mesh scaffolds after 1, 4 and 12 weeks of degradation in PBS and α-amylase solutions. Insets in **(b)** are magnified images of SEM images. Interconnectivity **(c)** and porosity **(d)** of SEVA-C fibre-mesh scaffolds as function of degradation time in PBS solution and in presence of α-amylase (pH 7.4, 37 ºC). A single asterisk (*) indicates a significant difference (p<0.05) for the

same material at different time points. A plus (+) indicates a significant difference (p < 0.05) between conditions for the same time point.

FIGURE 6 Compressive modulus of SEVA-C fibre-mesh scaffolds in the wet state as function of degradation time in PBS solution and in presence of α-amylase (pH 7.4, 37 ºC). A single asterisk (*) indicates a significant difference (p<0.05) for the same material at different time points. A plus (+) indicates a significant difference (p<0.05) between conditions for the same time point.

FIGURE 7 Viability **(a)** and proliferation **(b)** of SaOs-2 cells seeded on SEVA-C fibre mesh scaffolds for 1, 3, 7 and 14 days of culture determined by the MTS assay and DNA quantification, respectively. A single asterisk (*) indicates a significant difference (p<0.05) at different time points.

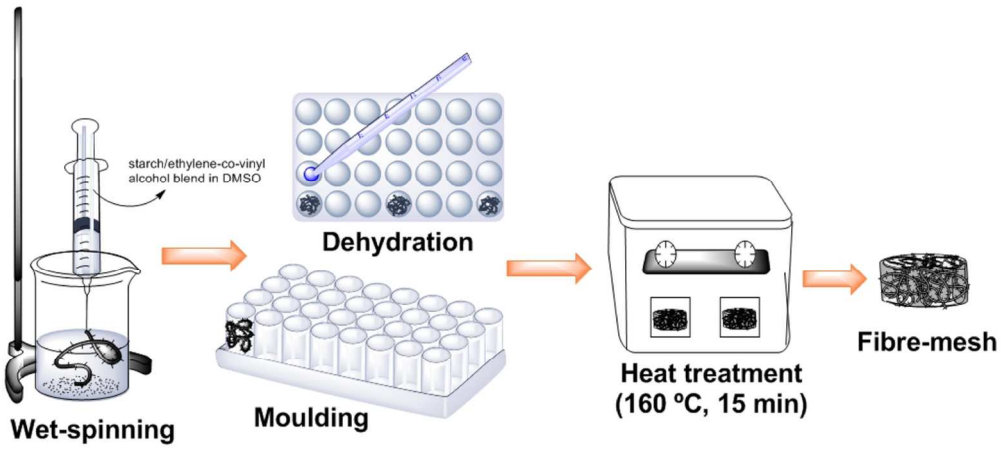

Schematic illustration of the setup for the production of the fibre-mesh scaffolds using wet-spinning technique
120x53mm (300 x 300 DPI)

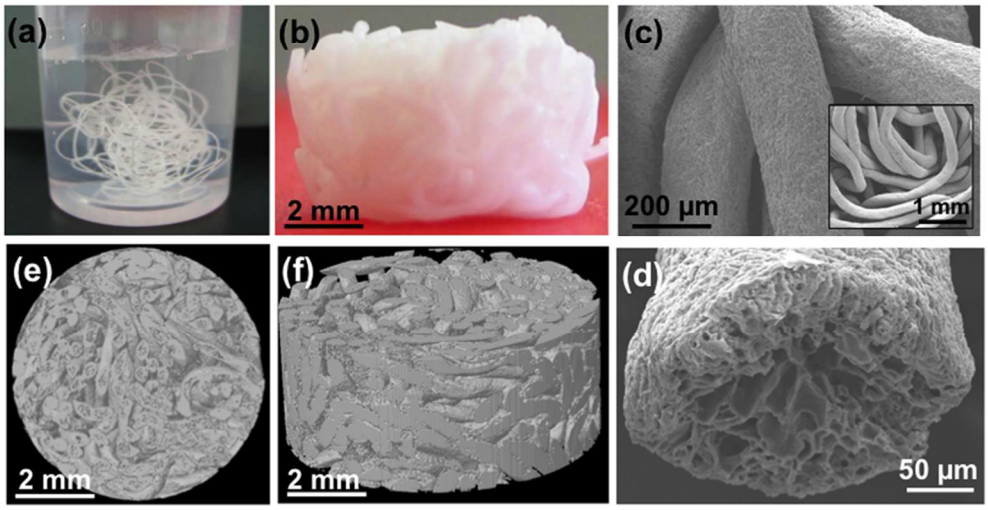

SEVA-C fibres after processing by wet-spinning (a) and after moulding into a 3D structure (b). SEM images of SEVA-C fibre mesh scaffolds (c) and fibre cross-section (d). Inset in (c) is lower magnification of SEM image. 2D (e) and 3D (f) visualizations obtained by µCT analysis.
91x53mm (300 x 300 DPI)

Initial	Immediately after compression	2 h after compression	24 h after compression
	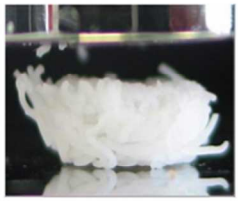		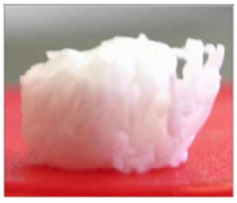
Height: 3.9 mm Ø = 7.8 mm	Height: 1.6 mm Ø = 9.2 mm	Height: 2.9 mm Ø = 8.2 mm	Height: 3.7 mm Ø = 7.9 mm

Scaffold dimensions in terms of height and diameter (Ø) before and after compression test (load cell of 1 kN; crosshead speed 2 mm/min; 60% strain).

86x39mm (300 x 300 DPI)

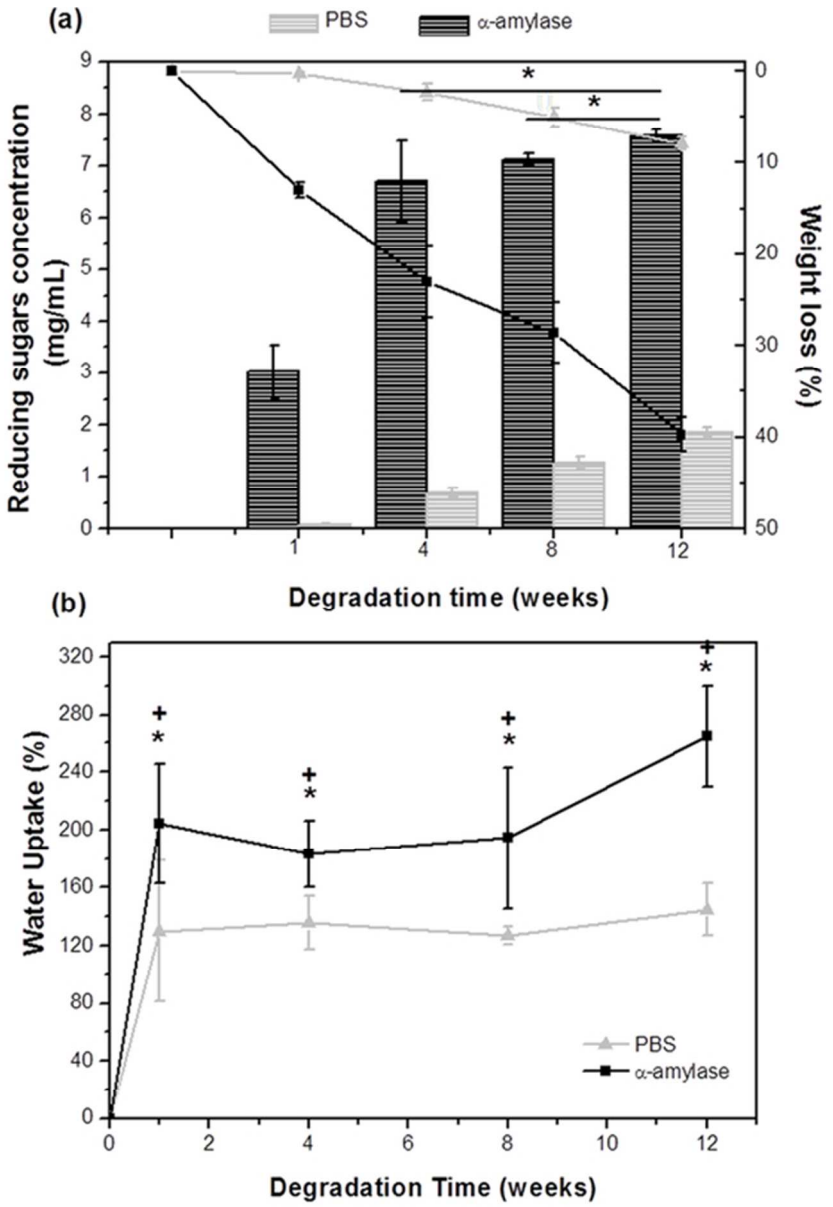

Degradation profile of the SEVA-C fibre-mesh scaffolds measured in terms of (a) weight loss (----) and reducing sugar concentration ( ) and (b) water uptake as function of degradation time in PBS solution (pH 7.4, 37 ºC) and in presence of α-amylase. A single asterisk (*) indicates a significant difference ($p<0.05$) for the same sample at different time points. A plus (+) indicates a significant difference ($p<0.05$) between conditions for the same time point.
48x68mm (300 x 300 DPI)

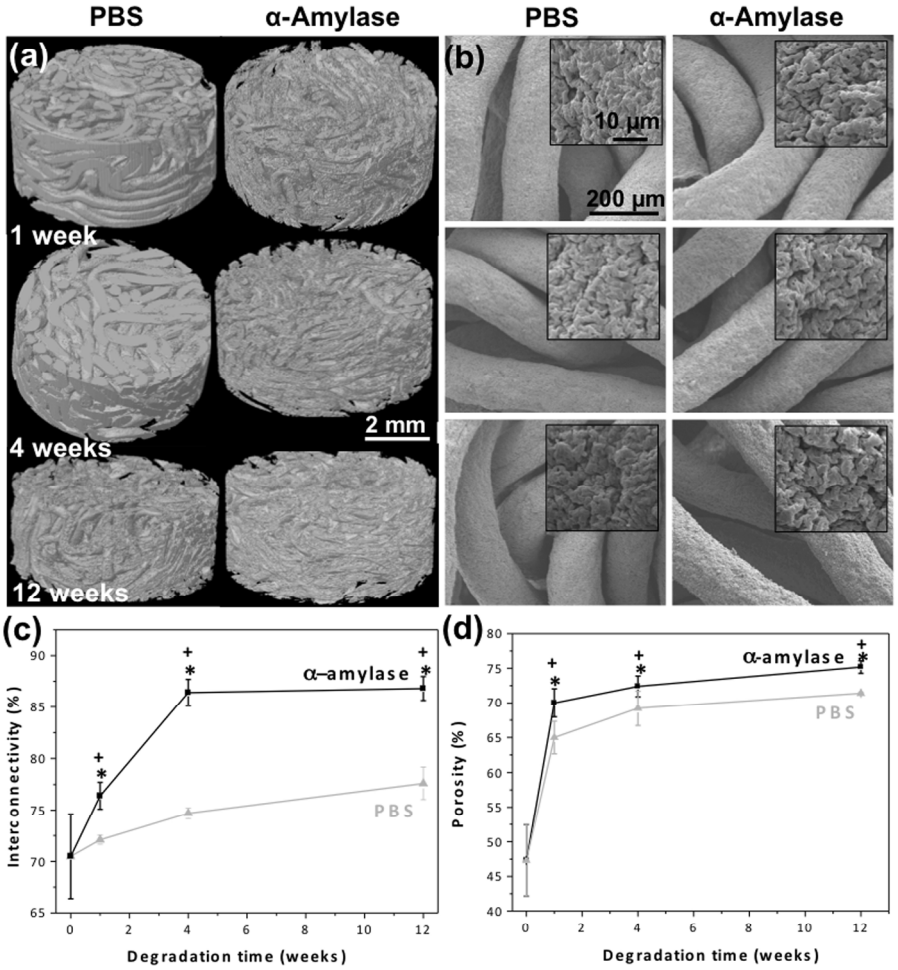

µCT (a) and SEM (b) images of SEVA-C fibre mesh scaffolds after 1, 4 and 12 weeks of degradation in PBS and α-amylase solutions. Insets in (b) are magnified images of SEM images. Interconnectivity (c) and porosity (d) of SEVA-C fibre-mesh scaffolds as function of degradation time in PBS solution and in presence of α-amylase (pH 7.4, 37 ºC). A single asterisk (*) indicates a significant difference ($p<0.05$) for the same material at different time points. A plus (+) indicates a significant difference ($p < 0.05$) between conditions for the same time point.
252x336mm (300 x 300 DPI)

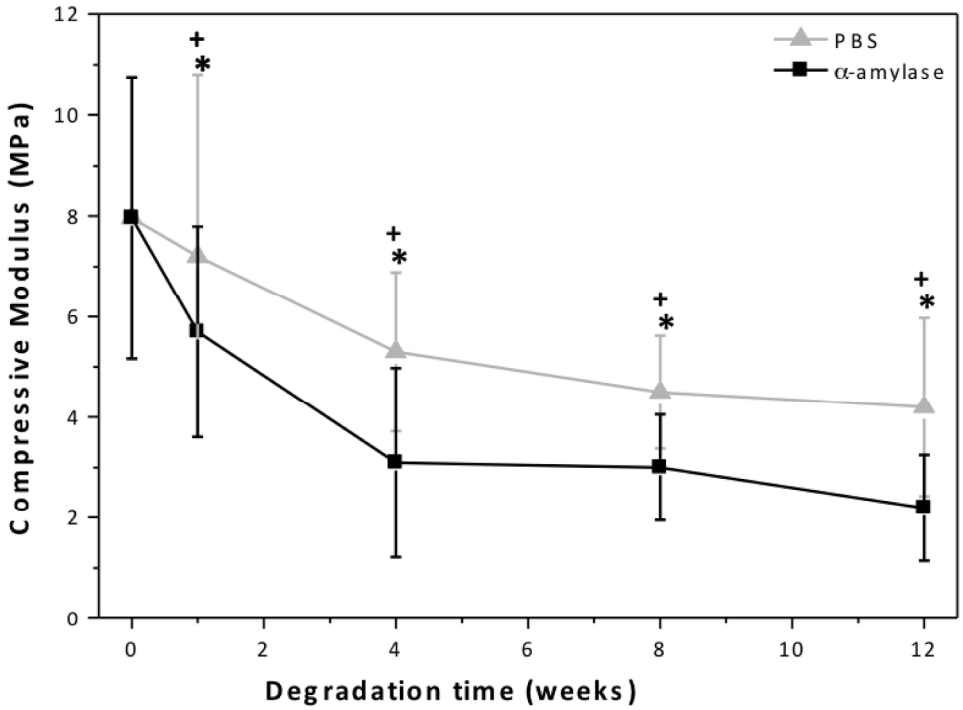

Compressive modulus of SEVA-C fibre-mesh scaffolds in the wet state as function of degradation time in PBS solution and in presence of α-amylase (pH 7.4, 37 ºC). A single asterisk (*) indicates a significant difference ($p<0.05$) for the same material at different time points. A plus (+) indicates a significant difference ($p<0.05$) between conditions for the same time point.
216x162mm (300 x 300 DPI)

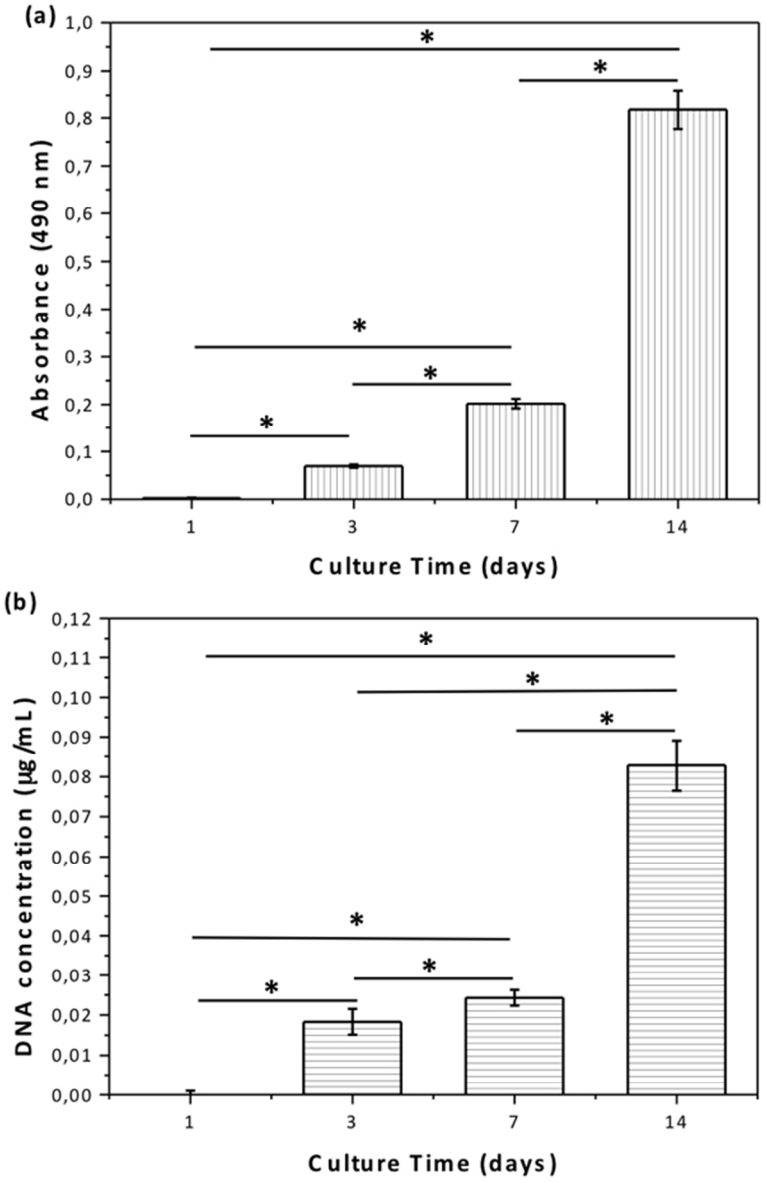

Viability (a) and proliferation (b) of SaOs-2 cells seeded on SEVA-C fibre mesh scaffolds for 1, 3, 7 and 14 days of culture determined by the MTS assay and DNA quantification, respectively. A single asterisk (*) indicates a significant difference ($p<0.05$) at different time points.